Tabular Wasserstein Autoencoder

Alex X. Wang, and Binh P. Nguyen

Abstract—Tabular data generation is a complex task due to its distinctive characteristics and inherent complexities. While Variational Autoencoders (VAEs) have been adapted from the computer vision domain for tabular data synthesis, their reliance on non-deterministic latent space regularization introduces limitations. The stochastic nature of VAEs can contribute to collapsed posteriors, yielding suboptimal outcomes and limiting control over the latent space. This characteristic also constrains the exploration of latent space interpolation. To address these challenges, we present the Tabular Wasserstein Autoencoder (TWAE), leveraging the deterministic encoding mechanism of Wasserstein Autoencoders (WAEs). This characteristic facilitates a deterministic mapping of inputs to latent codes, enhancing the stability and expressiveness of our model's latent space. This, in turn, enables seamless integration with shallow interpolation mechanisms like the synthetic minority oversampling technique (SMOTE) within the deep learning generation process. Specifically, TWAE is trained once to establish a low-dimensional representation of real data, and various latent interpolation methods efficiently generate synthetic latent points, achieving a balance between accuracy and efficiency. Extensive experiments consistently demonstrate TWAE's superiority, showcasing its versatility across diverse feature types and dataset sizes. This innovative approach, combining WAE principles with shallow interpolation, effectively leverages SMOTE's advantages, establishing TWAE as a robust solution for complex tabular data synthesis.

Index Terms—Deep neural networks, tabular data, tabular data synthesis, latent space interpolation, SMOTE

1 Introduction

The demand for high-quality tabular data is substantial, given its standing as one of the most prevalent and widely used data modalities across diverse fields [1], [2], [3]. With its structured format, comprising rows and columns, tabular data serves as a fundamental choice for representing information in databases, spreadsheets, and various data storage systems encountered in daily life. Despite its popularity, the challenges of data scarcity persist from multiple perspectives, including the lack of big data, the barrier of collecting specific classes of data, and privacy concerns that limit data accessibility [4]. Synthetic data emerges as a valuable solution to overcome these challenges, particularly when additional data is required, specific classes are needed, or privacy concerns restrict access to real datasets [5].

Training high-quality generative models for tabular data is challenging compared to other domains like computer vision and natural language processing. Recent literature highlights the dominance of traditional machine learning (ML) methods over deep learning (DL) techniques in this context, emphasizing the complexities inherent in tabular data, such as its heterogeneous data types and lack of inherent structure [6]. Consequently, the development of a robust deep representation and generation framework specifically for tabular data remains an open problem [7]. Models like Generative Adversarial Networks (GANs) and Variational Autoencoders (VAEs) often rely on stochastically generated latent variables, limiting control over the latent space and, consequently, the quality of generated data [8]. Despite limited comparisons with simple interpolation models like the synthetic minority over-sampling technique (SMOTE) [9], available evidence suggests that SMOTE is often challenging to outperform [10], [11]. This highlights the need for innovative DL approaches to address the unique challenges of tabular data synthesis.

Our study explores the Wasserstein Autoencoder (WAE) in addressing the intricate challenge of tabular data synthesis. The adoption of WAE in this domain provides dual advantages. Firstly, unlike standard GANs and VAEs, the introduction of a deterministic latent space proves notably advantageous [12]. Secondly, acknowledging the efficacy of SMOTE's shallow interpolation mechanism in the tabular data context, we seek to seamlessly integrate this approach into our DL process through latent space interpolation, leveraging the deterministic mapping of the latent space [13]. Both mechanisms form the foundation of our proposed model, the Tabular Wasserstein Autoencoder (TWAE), a streamlined architecture specifically tailored for tabular data synthesis. Our comprehensive experiments demonstrate the superior performance of this approach across diverse benchmark datasets. Specifically, the key contributions of our study are outlined as follows:

1) We conduct a comprehensive evaluation of key tabular data generation models, assessing their relative performance and computational efficiency across various tasks and datasets.
2) We present TWAE, a streamlined model specifically designed for generating tabular data, demonstrating its ability to handle heterogeneous data types.
3) We demonstrate the superior performance of TWAE compared to alternative methods tailored for tabular data. This includes statistical techniques, traditional ML algorithms, and recently proposed GAN-based and VAE-based models. Our analysis delves into the underlying factors contributing to this advantage across multiple datasets.
4) Although we recognize the effectiveness of shallow interpolation techniques such as SMOTE in producing synthetic data that is comparable to real data while using minimal computer resources, our study consistently demonstrates the superiority of

our proposed algorithm, especially when dealing with large datasets.

2 Related Work

2.1 Tabular data generation and its challenges

Data generation involves creating synthetic data points that closely resemble real data [14]. This process serves multiple purposes, including augmenting existing datasets, addressing data scarcity, enhancing privacy, and training/testing ML models [3]. In the context of generative modeling, algorithms are specifically crafted to learn underlying patterns and structures from a given dataset. Subsequently, these algorithms generate new samples that exhibit similar characteristics to the original data. Mathematically, consider a dataset of examples, $\{x_i | x_i \in \mathbb{R}, i = 1, \ldots, N\}$, sampled from a true data distribution, $\mathbb{P}$. The objective of a Deep Generative Model (DGM) is to construct deep neural networks (DNN) with parameters θ to define a distribution $p_\theta(x)$. The parameters θ are trained to ensure that the distribution $p_\theta(x)$ closely aligns with the true data distribution $\mathbb{P}$. Then one can use $p_\theta(x)$ to generate synthetic data.

The generation of tabular data, along with other forms of data, has become an important subject due to its growing use in addressing practical business issues [15]. However, generating synthetic tabular data is non-trivial due to its inherent complexities. Firstly, tabular data collection can be diverse and manual. It can also originate from various systems, leading to arbitrary dataset lengths and inconsistent features with missing values. Secondly, the numerical and categorical nature of tabular data poses challenges in both ML model training and evaluation. The encoding of categorical variables into a numeric format adds complexity, especially when features are derived from unrelated sources with differing units. Furthermore, conventional metrics such as the "Inception Score," designed for 2D image data, may not be well-suited for assessing the quality of synthetic tabular data [16], [17]. Lastly, the generation of tabular synthetic data is often driven by specific business questions, requiring specialized preprocessing and postprocessing steps. It is crucial to recognize that synthetic data created to enhance ML models differs significantly from data created for privacy preservation; each represents a distinct trade-off between data accuracy and privacy [18]. Addressing these intricacies in generative modeling for tabular data remains an open research frontier.

2.2 VAE

The VAEs is a probabilistic generative model designed for learning latent representations of data [19]. It comprises two main elements: an encoder network and a decoder network. Let x represent the observed data and z the latent variable. While the encoder function $q_\phi(z|x)$ estimates the posterior distribution of the latent variable given the data, the decoder function $p_\theta(x|z)$ approximates the conditional distribution of the data given the latent variable. Both q_ϕ and p_θ are parametrized by neural networks with parameters ϕ and θ, respectively. The objective of VAE is to maximize the Evidence Lower Bound (ELBO) on the log-likelihood of the observed data, which can be expressed as:

$$\log p_\theta(x) \geq \mathbb{E}_{q_\phi(z|x)}[\log p_\theta(x|z)] - \mathrm{KL}[q_\phi(z|x)||p(z)]. \quad (1)$$

The VAE loss function is typically expressed as the negative ELBO, as shown below:

$$\mathcal{L}_{\mathrm{VAE}} = -\mathbb{E}_{q(z|x)}[\log p(x|z)] + \mathrm{KL}[q(z|x)||p(z)], \quad (2)$$

where there are two main components:

- $\mathbb{E}_{q(z|x)}[\log p(x|z)]$ is the reconstruction term, and
- $\mathrm{KL}[q(z|x)||p(z)$ is the Kullback-Leibler (KL) divergence as a regularization term.

This loss function is designed to balance the trade-off between accurately reconstructing the input data and regularizing the latent space. However, using Kullback-Leibler (KL) divergence as a regularization term in generative models, notably VAEs, was reported with several issues. Firstly, KL divergence can lead to over-regularization and mode collapse, where the model overly restricts the latent pace [12]. It is also sensitive to the choice of the prior distribution and assumes a specific form, limiting its ability to capture complex latent structures [20]. Finally, KL divergence may result in loss reconstructions, face challenges with gradient vanishing during training, and introduce a trade-off between generation quality and regularization strength [21]. Given the issues above, Tolstikhin *et al*. [12] generalized the generative modeling to an optimal transport (OT) problem [22] and proposed a new family of regularized autoencoders, which is named Wasserstein Autoencoder (WAE).

2.3 WAE

Similar to VAE, WAE aims to minimize both the reconstruction cost and a regularization term, denoted as $D_z(P_z, Q_z)$, representing any arbitrary divergence metrics between Q_z and P_z. The general form of the loss function is expressed as:

$$\mathcal{L}_{\mathrm{WAE}} = \mathbb{E}_{q(z|x)}[\log p(x|z)] + \lambda \cdot D_z(q(z|x), p(z)), \quad (3)$$

where $\mathbb{E}_{q(z|x)}[\log p(x|z)]$ serves as the reconstruction term, $D_z(q(z|x), p(z))$ represents any arbitrary divergence metrics, and $\lambda > 0$ is a hyperparameter. Tolstikhin *et al*. [12] proposes two specific regularizers: the Maximum Mean Discrepancy (MMD) and adversarial training, to address issues and provide more flexibility in latent space modeling. It is noteworthy that when adversarial training is employed, it aligns with the Adversarial Autoencoder proposed by Zhao *et al*. [20]. Kolouri *et al*. [23] propose an alternative method that uses the Sliced-Wasserstein distance to transform the latent distribution of an autoencoder into a prior distribution that may be sampled. Subsequent to this unique approach, recent state-of-the-art models have undergone significant development, as demonstrated by works such as Yi *et al*. [24].

The WAE leverages the Wasserstein distance to establish a direct and deterministic mapping from input data to the latent space, offering a solution to the inherent stochasticity of latent variables in both GANs and VAEs [12]. This deterministic mapping not only addresses the issue of randomness but also allows for the inclusion of latent space interpolation, a well-recognized technique in computer vision and natural language processing. This aligns with the proven effectiveness of shallow interpolation methods such as SMOTE in the domain of tabular data. This versatility

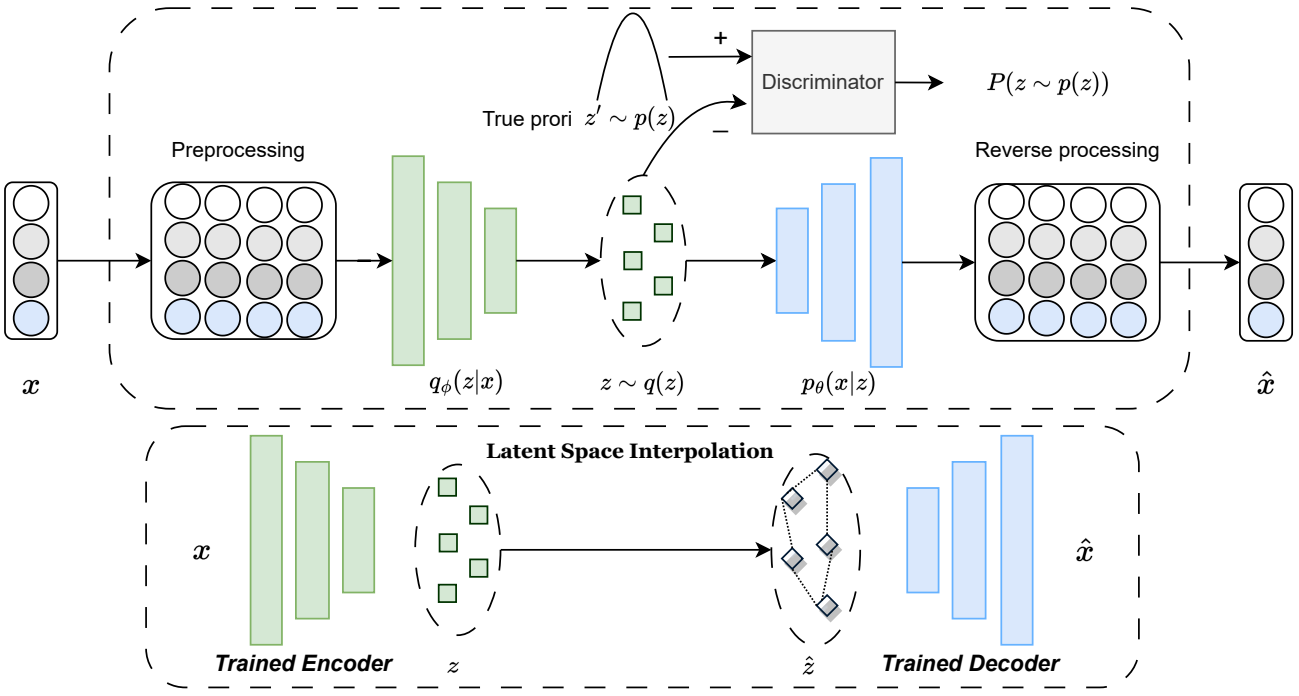

Fig. 1. Illustrating the TWAE with latent space interpolation: During the training phase, each data sample x undergoes preprocessing and is subsequently transformed by the encoder, resulting in a mapping to a latent space vector z. Subsequently, the encoded latent space vector z is utilized as an input for the decoder, which engages in a reconstruction process incorporating both reconstruction loss and regularization loss. During the generation phase, a synthetic latent space vector $\hat{z}$ is generated through latent space interpolation on the encoded latent space vector z. This synthetic vector is then fed into the trained decoder to generate synthetic data, followed by reverse processing to return the data to its original format, $\hat{x}$.

allows WAE to extend its applicability beyond traditional image and language data to diverse domains, including tabular datasets.

3 TWAE: Tabular Wasserstein Autoencoder

3.1 Description

TWAE is constructed based on an encoder/decoder/critic framework, incorporating a latent space interpolation method and a loss function comprising both a reconstruction loss and a regularization term. The high-level flow of TWAE is illustrated in Figure 1, and an overview of the pseudo-code for TWAE is presented in Algorithm 1. The TWAE process involves two primary stages: (1) fine-tuning a WAE to establish a smooth and controllable latent space, and (2) sampling from latent space interpolations generated by the fine-tuned WAE to produce synthetic tabular data. The subsequent sections delve into the specific procedures of each component, providing a detailed exploration of the fine-tuning and sampling processes. The section concludes with a concise summary of our approach.

3.2 Preprocessing

Following the approach outlined in [25], a reversible preprocessing step is employed both before model training (converting original data into a machine-readable format) and after data generation (transforming synthetic data back into the original format). To handle continuous variables, a variational Gaussian mixture model (VGM) is utilized to address non-Gaussian and multimodal distributions. Initially, the model estimates the number of modes, denoted as m, and subsequently fits a Gaussian mixture. The values are normalized within each mode, and a mode is represented as a one-hot vector $\beta_{i,j} = [0, 0, ..., 1]$, while $\alpha_{i,j}$ denotes the normalized value. Here, i represents the ith column, and j represents the jth row. Consequently, the original continuous variables for row j can be expressed as $\alpha_{1,j} \oplus \beta_{1,j} \oplus ... \oplus \alpha_{n_c,j} \oplus \beta_{n_c,j}$, where $\oplus$ signifies concatenation. For categorical features, one-hot encoding is employed to convert each unique categorical element into its binary vector column. This transformation leads to discrete columns $D_1, ..., D_{n_d}$ being converted into one-hot vectors $d_1, ..., d_{n_d}$, where the ith one-hot vector is denoted as $d_i = [d_i^{(k)}]$ for $k = 1, ..., C_i$ (representing categories in the ith column). Hence, the original categorical variables for row j can be represented as $d_{1,j} \oplus ... \oplus d_{n_d,j}$. As a result, the initial jth row, denoted as r_j, can be effectively represented as the concatenation of the processed numerical and categorical variables. This representation is ready to be fed into the subsequent DGMs:

$$r_j = \alpha_{1,j} \oplus \beta_{1,j} \oplus ... \oplus \alpha_{n_c,j} \oplus \beta_{n_c,j} + d_{1,j} \oplus ... \oplus d_{n_d,j}. \quad (4)$$

3.3 Enhanced loss function

Tolstikhin *et al.* [12] proposed two loss functions: $\mathcal{L}_{\text{WAE-MMD}}$ and $\mathcal{L}_{\text{WAE-GAN}}$, each exhibiting distinct advantages and drawbacks. WAE-MMD effectively addresses mode collapse, enhancing diversity in generated samples, while

Algorithm 1 Tabular Wasserstein Autoencoder

Input: Real data samples $\{x(i)\}_{i=1}^{m}$, learning rates $\alpha_{\text{enc}}, \alpha_{\text{dec}}, \alpha_{\text{dis}}$, GAN-based regularization coefficient λ_1, MMD-based regularization coefficient λ_2
Initialize: Autoencoder parameters ϕ, θ, Discriminator parameters ψ
for each training iteration **do**
  Sample $x(i)$ from the training set
  Sample $z'(i)$ from the true prior p_z
  Sample z from $q_\phi(z|x)$
  Update the Critic (ψ) **:**
  Compute the critic loss:
  $L_{\text{cri}} \leftarrow -\frac{1}{m}\sum_{i=1}^{m} f_w(z(i)) + \frac{1}{m}\sum_{i=1}^{m} f_w(z'(i))$
  Update critic parameters:
  $\psi \leftarrow \psi - \alpha_{\text{cri}} \nabla_\psi (L_{\text{cri}})$
  Train the encoder/decoder (ϕ, θ)**:**
  Compute the reconstruction loss:
  $L_{\text{rec}} \leftarrow -\frac{1}{m}\sum_{i=1}^{m} \log p_\theta(x(i)|z(i))$
  Compute the regulation loss(es):
  $L_{\text{reg}} \leftarrow D_z(q(z|x), p(z))$
  Update encoder and decoder parameters:
  $\phi \leftarrow \phi - \alpha_{\text{enc}} \nabla_\phi (L_{\text{rec}} + \lambda L_{\text{reg}})$
  $\theta \leftarrow \theta - \alpha_{\text{dec}} \nabla_\theta (L_{\text{rec}} + \lambda L_{\text{reg}})$
end for

WAE-GAN introduces a smoother latent space and improves image quality. To capitalize on the benefits of both approaches, our study introduces a novel hybrid loss function. By combining the strengths of WAE-MMD and WAE-GAN, we anticipate achieving a more stable training process, effectively mitigating mode collapse and training instability. This hybrid approach aims to strike a balance between stability, diversity, and quality in generative modeling. The loss function in TWAE comprises three key terms: a reconstruction loss L_{rec}, a regularization term from MMD L_{reg_m}, and an adversarial regularization term from GAN L_{reg_g}. The impact of each component can be adjusted using corresponding hyperparameters λ_m and λ_g ($\lambda > 0$). It is essential to highlight that there are numerous possibilities for this regularization term, enhancing the adaptability of our algorithm. The proposed loss function is articulated as follows:

$$\mathcal{L}_{\text{TWAE}} = L_{\text{rec}} + \lambda_m \cdot L_{reg_m} + \lambda_g \cdot L_{reg_g}, \tag{5}$$

where:

$$\begin{aligned} L_{\text{rec}} &\leftarrow -\mathbb{E}_{q(z|x)}[\log p(x|z)], \\ L_{reg_m} &\leftarrow \text{MMD}(q(z), p(z)), \\ L_{reg_g} &\leftarrow \text{W}_c(q(z|x), p(z)). \end{aligned} \tag{6}$$

When λ_{reg_g} is set to 0, $\mathcal{L}_{\text{TWAE}}$ coincides with that of $\mathcal{L}_{\text{WAE-MMD}}$, which is given by:

$$\mathcal{L}_{\text{WAE-MMD}} = -\mathbb{E}_{q(z|x)}[\log p(x|z)] \quad + \lambda \cdot \text{MMD}(q(z), p(z)). \tag{7}$$

Here, $\text{MMD}(q(z), p(z))$ represents the Maximum Mean Discrepancy between the approximate posterior $q(z)$ and the prior $p(z)$, as delineated below [26]. The parameter λ serves as a hyperparameter governing the intensity of the MMD regularization.

$$\begin{aligned} &\text{MMD}^2(q(z), p(z)) = \|\mu_q - \mu_p\|_{\mathcal{F}}^2 \\ &= \frac{1}{n(n-1)}\sum_{i \neq j} k(z_i, z_j) + \frac{1}{n(n-1)}\sum_{i \neq j} k(z_i', z_j') - \frac{2}{nn}\sum_{i,j} k(z_i, z_j'), \end{aligned} \tag{8}$$

where $k(.,.)$is a positive definite kernel function.

$$k(q, p) = \exp\left(-\frac{\|z - z'\|^2}{2\sigma^2}\right). \tag{9}$$

When λ_{reg_m} is set to 0, $\mathcal{L}_{\text{TWAE}}$ coincides with that of $\mathcal{L}_{\text{WAE-GAN}}$, which is given by:

$$\mathcal{L}_{\text{WAE-GAN}} = -\mathbb{E}_{q(z|x)}[\log p(x|z)] \quad + \lambda \cdot \text{W}_c(q(z|x), p(z)), \tag{10}$$

where $\text{W}_c(q(z|x), p(z))$ is the Wasserstein distance with regularization and λ is a hyperparameter controlling the strength of the Wasserstein regularization.

3.4 Latent space interpolation for data generation

Latent space interpolation is a well-investigated concept in generative modeling, particularly within the domain of computer vision [27]. In the context of DGMs, latent space interpolation offers several advantages for data generation [28]. It facilitates smoother and more controlled data generation by allowing gradual transitions between data samples, and it aids in a deeper understanding of the underlying data structure. Such enhancements in data representation contribute to more meaningful and realistic data generation, as noted by recent studies [13]. While latent space interpolation has succeeded in the DL domain, shallow interpolation methods like SMOTE have proven effective in the tabular data domain. Leveraging our enhanced loss function and model architecture, we achieve a deterministic latent space, paving the way for exploring this technique in tabular data generation—a novel contribution in this paper. We employ three distinct approaches to introduce noise into the latent space through interpolation [29], as depicted in Figure 2 below. It is crucial to highlight that these approaches constitute only a subset of the diverse methods available for latent space interpolation. The first approach aligns with the concept of SMOTE, generating synthetic latent variables along the path between a randomly selected latent variable and one of its neighbors. The second method, termed the triangular mechanism, entails selecting n observations z, to generate $z_s = \lambda_1 z_1 + ... + (1 - \lambda_1 - ... - \lambda_{n-1}) z_{n-1}$, where $\lambda_i \sim U(0, 1)$. The third method, the hyper-rectangle mechanism, works in a balanced manner similar to the first and second, using two latent variables to generate a new latent variable within a rectangle area.

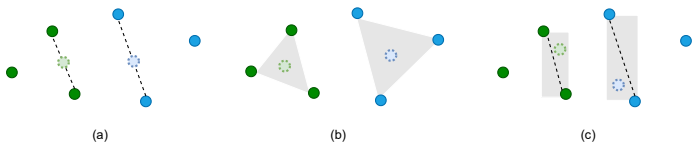

Fig. 2. Illustration of latent interpolation used in this study. **a** Within-class interpolation, **b** triangular interpolation, **c** hyper-rectangle interpolation

4 Experimental Study

We undertake a series of experiments to assess the performance of TWAE, utilizing a diverse range of data quality metrics. Our goal is to deliver a reliable evaluation outcome by establishing a unified and comprehensive framework for the assessment of tabular data synthesis techniques. To encourage further research and ensure reproducibility, our code is made publicly available in the GitHub repository[1].

4.1 Datasets

To systematically evaluate the performance of our proposed algorithm, we curated a comprehensive set of 16 real-world public datasets for comparison against state-of-the-art data synthesis algorithms. These datasets exhibit variations in size, characteristics, number of features, and data distributions. Many of these datasets have been previously employed for evaluating tabular models in prior studies [11], [25], [30]. The complete list of datasets and their properties is detailed in Table 1. To avoid data leakage, we partitioned all datasets into 80% for training and 20% for testing purposes. All models were trained on the same training data samples with their default hyperparameters. Results were averaged and reported based on five trials conducted with different random seeds [31].

TABLE 1
Statistics of datasets used in this study. #S stands for the number of samples, #N stands for the number of numerical columns, #c stands for the number of categorical columns and IR stands for Imbalance Ratio.

Abbr	Name	#S	#N	#C	IR
CR	credit-g	1000	3	18	2.33
SI	sick	3000	5	18	13.43
JS	jasmine	3000	8	137	1.00
NS	national-longitudinal-survey	4908	5	12	1.65
KD	KDDCup09_upselling	5128	27	21	1.00
EY	eye_movements	7608	17	6	1.00
DE	default-of-credit-card	13272	14	8	1.00
NC	NewspaperChurn	15855	3	14	4.22
CO	compass	16644	5	13	1.00
LA	law-school-admission	20800	2	9	2.11
NO	nomao	34465	56	63	2.50
MV	mv	40768	6	4	1.48
BM	Bank-Marketing	45211	7	10	7.55
AD	adult	48842	5	10	6.43
DB	diabetes	70692	3	19	1.00
CI	Census-Income	299285	9	33	15.12

4.2 Reference tabular data synthesis models

A variety of methods exist for generating synthetic tabular data, each with its own unique advantages and limitations [29]. Perturbation-based models, such as linear or non-linear transformations, are straightforward and suitable for small datasets with continuous features but lack data privacy guarantees and face challenges with categorical features and larger datasets. Statistical distribution-based approaches simulate data based on known distributions, capturing statistical properties but often assuming feature independence. Distance-based methods, typified by SMOTE, are effective for oversampling minority classes, with variants like ADASYN [32] and SMOTENC [33] addressing categorical data. Deep Generative Models (DGMs) are versatile in generating diverse data types but encounter difficulties when handling discrete and categorical data. Recent research has produced numerous models, including tabular VAEs, GAN-based models, and Diffusion-based models, such as TVAE and TabDDPM. In this study, we conducted a comprehensive comparison against state-of-the-art tabular synthetic data models from statistical, ML, and DL models, including Copula [34], Synthpop [35], SMOTE [9], and its variants: ADASYN, along with TVAE, CTGAN [25], CopulaGAN [36], CTABGAN+ [30], and TabDDPM [11].

1. https://github.com/coksvictoria/TWAE

4.3 Evaluation metrics

Consistent with previous studies [14], [37], [38], we evaluated the quality of synthetic data along three dimensions: ML utility, statistical similarity, and privacy. Each evaluation aspect is supplemented with visualization aids.

4.3.1 *ML utility*

Regarding ML utility, our principal evaluation metric was the F1 score, consistent with common practice in previous studies [11], [25]. Additionally, we included the Area under the Precision-Recall curve (PR-AUC) and the Area under the Receiver Operating Characteristic Curve (ROC-AUC) to offer a more comprehensive assessment of our experiments. While the ROC-AUC considers sensitivity and specificity across various decision boundaries, providing insights into the overall model performance, the F1 score and PR-AUC, which concentrate on the precision-recall trade-off, prove more informative in scenarios with imbalanced data [39]. We trained classification models and evaluated their performance on a distinct holdout test dataset to mitigate information leakage.

We interpreted the results from two perspectives: performance consistency and ranking consistency [3], [37], [40], [41]. Performance consistency anticipates that models trained on high-quality synthetic data should be equally competitive as, or even outperform, those trained on real data. Ranking consistency means if algorithm A performs better than algorithm B on real data, then the ranking should still hold on the synthetic data. We employed six widely used classification methods, namely Multi-Layer Perceptron (MLP), k-Nearest Neighbours (k-NN), Logistic Regression (LR), Decision Tree (DT), Random Forest (RF), and Light Gradient Boosting Machine (LightGBM) [11], [25], [42]. The reason for choosing these methods is based on the variety of algorithmic paradigms they represent. This set of algorithms covers a wide range of model complexities, from basic linear models to advanced ensemble approaches. Furthermore, these algorithms exhibit different levels of responsiveness to class imbalance. Our goal is to thoroughly evaluate the effectiveness of each tabular data synthesis procedure in various contexts by incorporating a wide range of classification algorithms. To ensure a fair comparison, we utilized the default hyperparameters for all the classification algorithms [31].

4.3.2 *Statistical similarity*

For statistical similarity, we employed three groups of metrics commonly used in previous studies: column-wise met-

rics (univariate), pair-wise column correlation (bivariate), and table-level metrics (multivariate) [11], [43], [44].

For column-wise metrics, we utilized the Kullback-Leibler divergence (KLD), Jensen-Shannon divergence (JSD), and Wasserstein distance (WD) to assess synthetic data from a univariate distribution perspective [30], [45]. It is worth noting that both KLD and WD are components of the loss functions in VAE and WAE, as presented earlier.

KLD between two distributions P and Q, denoted as $D_{KL}(P \parallel Q)$, is defined as follows:

$$D_{KL}(P \parallel Q) = \int_x p(x) \log \frac{p(x)}{q(x)} dx, \tag{11}$$

where $p(x)$ and $q(x)$ are the probability density functions, respectively. It is noteworthy that KLD is asymmetric with a range of [0, $+\infty$), indicating that $D_{KL}(P \parallel Q) \neq D_{KL}(Q \parallel P)$. A lower value signifies closer similarity between two distributions.

JSD is the symmetric counterpart of KLD and is bounded between [0,1]. It is defined as:

$$D_{JS}(P|Q) = \frac{1}{2} D_{KL}(p|\frac{p+q}{2}) + \frac{1}{2} D_{KL}(q|\frac{p+q}{2}). \tag{12}$$

JSD offers two advantages over KLD. Firstly, it is symmetric, meaning $D_{JS}(P \parallel Q) = D_{JS}(Q \parallel P)$. Secondly, it is bounded between 0 and 1 (for log base 2), providing a smoothed and normalized version of KLD [46].

WD is another commonly used distance metric and can be mathematically defined as:

$$W(P, Q) = \inf_{\gamma \sim \Pi(p,q)} \mathbb{E}_{(x,y)\sim\gamma}[|x - y|], \tag{13}$$

where $\Pi(p, q)$ is the set of all possible joint probability distributions between p and q, and γ denotes a dirt transport plan. Specifically, $\gamma(x, y)$ represents the percentage of dirt that should be transported from point x to y to make x follow the same probability distribution as y [47].

In evaluating the column pair-wise statistical similarity between real and synthetic datasets, correlation analysis is a commonly used metric. The choice of correlation coefficients depends on the types of variables involved [3]. Specifically, for continuous-to-continuous variables, Pearson correlation coefficients were employed, and for continuous-to-nominal variables, correlation ratios were used. Point-biserial correlation was applied for continuous and dichotomous variables, while nominal-to-nominal associations, including dichotomous variables, were assessed using Cramer's V. Additionally, for dichotomous-to-dichotomous variables, the phi coefficient or Matthews Correlation Coefficient (MCC), was utilized. All correlation coefficients range from 0 to 1, with 0 indicating no correlation and 1 representing absolute certainty. After computing the correlation coefficients for both real and synthetic data, we applied the Kolmogorov-Smirnov (KS) test to them and reported the p-value, where a higher value is considered better. Moreover, we visually presented the absolute differences in these bivariate correlations in a heatmap, facilitating the comparison between real and synthetic datasets.

Finally, we employed the density and coverage scores proposed in [48] to gauge the overall fidelity and diversity of synthetic data. While coverage is constrained to a range between 0 and 1, density has no upper bound; nevertheless, higher values indicate better performance in both cases. The density score is computed as the average fraction of synthetic samples Y_j within the k-nearest neighbors'spheres centred at real samples X_i, indicating how well the synthetic data captures local neighborhoods in comparison to the real data. The formula is shown below:

$$\text{density} = \frac{1}{kM} \sum_{j=1}^{M} \sum_{i=1}^{N} 1_{Y_j \in B(X_i, \text{NND}_k(X_i))}, \tag{14}$$

where k means the number of nearest neighbors, M is the number of synthetic samples, N is the number of real samples. $1_{Y_j \in B(X_i, \text{NND}_k(X_i))}$ is an indicator function, which equals to 1 if Y_j falls within the sphere, 0 otherwise.

The coverage score is calculated as the fraction of real samples X_i for which there exists at least one synthetic sample Y_k within the k-nearest neighbors' spheres, indicating how well the synthetic data covers the space occupied by the real data:

$$\text{coverage} = \frac{1}{N} \sum_{i=1}^{N} \mathbf{1}\exists j \text{ s.t. } Y_j \in B(X_i, \text{NND}_k(X_i)). \tag{15}$$

4.3.3 Privacy

Privacy risks are multifaceted and stem from the possibility of disclosing sensitive information, threatening the privacy and confidentiality of individuals or entities represented in the data. Assessing privacy risks in synthetic data normally involves considering potential vulnerabilities when attackers have access to the synthetic dataset without knowledge of the underlying generative models [41].

A straightforward method involves checking for identical matches, specifically identifying records from the training dataset that also exist in the synthetic dataset [49]. The notion of identical matches is often extended to measure the distance to the closest records (DCR), which computes the distance between each synthetic sample and the most similar original record [50]. A lower DCR signifies a closer resemblance of synthetic data to real data. However, this metric cannot be used in isolation, as a high DCR indicates a lower privacy risk but may also suggest poor data quality in the synthetic data. To address this limitation, we incorporated another metric to evaluate the distinguishability of synthetic data from real data.

In this study, we employed ML detectability as a privacy measure, utilizing the propensity score [51]. To achieve this, the metric involves shuffling real and synthetic data together with flags indicating whether the data is real or synthetic. An ML model is then cross-validated to predict these flags, and the ability to discriminate is converted into a score [52]. As shown in the equation below, we used the $propsensityMSE$ score where the mean squared difference of the probability (propensity score) and 0.5 was calculated. We normalized it by dividing it by 0.25 to yield a range of [0,1]. A score of 0 implies that the synthetic data is indistinguishable from real data, while a score of 1 indicates that real and synthetic data are entirely distinguishable. In an ideal scenario, high-quality synthetic data should exhibit a low DCR and a high $propensityMSE$, indicating proximity to real data without just taking replication, thus minimizing privacy risks.

TABLE 2
F1 score, ROC-AUC and PR-AUC computed w.r.t. 16 datasets. **Bold** represents the best score on each dataset for each metric.

F1-Score	CR	SI	JS	NS	KD	EY	DE	NC	CO	LA	NO	MV	BM	AD	DB	CI	Ranking
SMOTE	0.5819	0.7653	0.0923	0.7976	0.4978	0.5592	0.4266	0.1067	0.6782	0.7399	0.8697	**0.9553**	0.1682	0.4333	0.7339	0.2844	5.5
ADASYN	0.5988	0.7758	0.0747	0.8090	0.4757	0.5276	0.4485	0.0997	0.6726	0.7442	0.8587	0.9537	0.1836	0.4484	**0.7348**	0.2989	5.4
Synthpop	0.4985	0.0007	0.1608	0.8899	0.6254	**0.6195**	0.3259	0.1056	0.3601	0.6888	0.7450	0.9166	0.2821	0.2828	0.0384	0.0573	5.4
Copula	0.7677	0.4360	0.0169	0.7870	0.5513	0.1249	0.5820	0.0623	0.2696	0.6865	0.8303	0.8796	0.0719	0.0957	0.5403	0.0195	5.1
CTGAN	0.7686	0.4797	0.0149	0.7617	0.5191	0.5081	0.5897	0.2221	0.6017	0.7535	0.8313	0.9126	0.4153	0.4463	0.6276	0.3563	4.5
CopulaGAN	0.7475	0.7555	0.0104	0.7233	0.5437	0.4624	0.6419	0.2558	0.6755	0.6567	0.8795	0.9296	0.2909	0.4606	0.6987	0.4171	4.0
TVAE	0.7750	0.7780	0.1429	0.9241	0.6307	0.5262	0.6481	**0.3372**	0.6422	0.7497	0.9407	0.9267	0.4311	0.4636	0.6774	0.2204	3.6
CTABGAN+	0.7765	0.7853	0.1405	0.9285	0.6496	0.4409	0.5926	0.2583	0.6665	0.7749	0.9400	0.9162	0.4086	0.3966	0.6710	0.3139	3.4
TabDDPM	0.7895	0.7781	0.1806	0.9311	0.6527	0.4972	0.6109	0.2718	0.6594	0.7629	0.9449	0.9272	0.4271	0.4342	0.6755	0.3303	2.7
TWAE	**0.7930**	**0.7943**	**0.2390**	**0.9405**	**0.6628**	0.5149	**0.6504**	0.3049	**0.6809**	**0.7862**	**0.9451**	0.9501	**0.4575**	**0.5372**	0.7248	**0.4535**	1.6
Real	0.7987	0.7909	0.2539	0.9540	0.6399	0.5392	0.6153	0.3157	0.7032	0.7857	0.9685	0.9683	0.4254	0.5228	0.7319	0.4679	

ROC-AUC	CR	SI	JS	NS	KD	EY	DE	NC	CO	LA	NO	MV	BM	AD	DB	CI	Ranking
SMOTE	0.6215	0.8132	0.7105	0.9159	0.6886	0.5842	0.6815	0.6526	0.7215	0.6811	0.8169	0.9719	0.7809	0.7186	0.7812	0.8283	5.5
ADASYN	0.6349	0.8201	**0.7134**	0.9167	0.6911	**0.5876**	0.6813	0.6471	0.7223	0.6843	0.7977	**0.9726**	0.7770	0.7280	**0.7823**	0.8312	5.6
Synthpop	0.3994	0.1036	0.7103	0.9095	**0.6952**	0.5178	0.5613	0.5400	0.5879	0.5232	0.7791	0.9412	0.6606	0.6026	0.4289	0.6185	5.8
Copula	0.5509	0.7310	0.5763	0.7694	0.6183	0.5284	0.6196	0.5609	0.6700	0.5555	0.8265	0.9140	0.6879	0.5688	0.7367	0.6438	5.4
CTGAN	0.4948	0.4981	0.5090	0.7370	0.5689	0.5311	0.5725	0.6373	0.6737	0.6516	0.7350	0.9415	0.8037	0.7251	0.7578	0.8353	4.9
CopulaGAN	0.5007	0.8126	0.5064	0.7172	0.5245	0.5422	0.6128	0.6177	0.7087	0.6061	0.8149	0.9511	0.7826	0.7266	0.7594	0.8569	4.4
TVAE	0.6356	0.8167	0.7345	0.9293	0.6898	0.5458	0.6827	0.6754	0.7024	0.6306	0.9468	0.9468	0.7966	0.7415	0.7472	0.7928	3.8
CTABGAN+	0.6480	0.8178	0.7337	0.9308	0.6934	0.5483	0.6812	0.6651	0.7072	0.6548	0.9447	0.9388	0.7926	0.7280	0.7495	0.8139	3.5
TabDDPM	0.6498	0.8140	0.7374	0.9340	0.6920	0.5444	**0.6877**	0.6803	0.7105	0.6570	**0.9520**	0.9408	0.8060	0.7412	0.7499	0.8240	2.8
TWAE	**0.6624**	**0.8196**	0.7603	**0.9417**	0.6775	0.5486	0.6795	**0.7055**	**0.7314**	**0.6862**	0.9508	0.9651	**0.8265**	**0.7756**	0.7822	**0.8800**	2.1
Real	0.6706	0.8328	0.7902	0.9532	0.7102	0.6221	0.6750	0.7238	0.7579	0.6895	0.9786	0.9781	0.8357	0.7719	0.7855	0.8798	

PR-AUC	CR	SI	JS	NS	KD	EY	DE	NC	CO	LA	NO	MV	BM	AD	DB	CI	Ranking
SMOTE	0.7798	0.2480	0.7529	0.9358	0.6767	0.5692	0.6598	0.3439	0.6928	0.8023	0.8914	0.9780	0.3896	0.5443	0.7412	0.4410	5.5
ADASYN	0.7884	0.2479	**0.7586**	0.9369	0.6769	**0.5742**	0.6608	0.3370	0.6950	**0.8047**	0.8809	**0.9789**	0.3841	0.5449	0.7423	0.4425	5.7
Synthpop	0.5631	0.1923	0.1043	0.9314	**0.6823**	0.5160	0.5443	0.2571	0.5764	0.6984	0.8650	0.9614	0.2098	0.3981	0.4660	0.1729	6.0
Copula	0.7332	0.1107	0.6902	0.8253	0.6108	0.5250	0.5964	0.2442	0.6488	0.7169	0.8958	0.9260	0.2556	0.3044	0.7050	0.1082	5.7
CTGAN	0.6976	0.0799	0.5070	0.8032	0.5560	0.5262	0.5628	0.3074	0.6453	0.7816	0.8449	0.9481	0.3669	0.5049	0.7225	0.3391	5.2
CopulaGAN	0.7016	0.0810	0.7543	0.7867	0.5218	0.5336	0.5839	0.2976	0.6825	0.7485	0.8908	0.9578	0.3508	0.5046	0.7230	0.4294	4.7
TVAE	0.7893	0.2440	0.7539	0.9414	0.6758	0.5379	0.6555	0.3555	0.6789	0.7649	0.9682	0.9548	0.3458	0.5115	0.7103	0.3518	4.2
CTABGAN+	0.7934	0.2324	0.7532	0.9416	0.6781	0.5401	0.6572	0.3468	0.6802	0.7807	0.9664	0.9479	0.3305	0.5110	0.7129	0.3934	3.8
TabDDPM	0.7982	0.2496	0.7538	0.9452	0.6755	0.5375	**0.6626**	0.3639	0.6871	0.7835	0.9709	0.9501	0.3425	0.5245	0.7126	0.4138	3.1
TWAE	**0.8044**	**0.2660**	0.7576	**0.9510**	0.6544	0.5423	0.6552	**0.4010**	**0.7065**	0.8036	**0.9710**	0.9697	**0.4290**	**0.5788**	**0.7440**	**0.4638**	2.1
Real	0.8055	0.3096	0.7729	0.9628	0.6919	0.6022	0.6524	0.4250	0.7322	0.8065	0.9866	0.9846	0.4447	0.5908	0.7470	0.4989	

TABLE 3
F1 score, ROC-AUC and PR-AUC computed w.r.t. six classification models. **Bold** represents the best result on each classification model for each metric. * denotes that the synthetic result is superior to that of real data.

	F1						ROC-AUC						PR-AUC					
	MLP	KNN	LR	DT	RF	LGBM	MLP	KNN	LR	DT	RF	LGBM	MLP	KNN	LR	DT	RF	LGBM
SMOTE	0.5164	0.5076	0.4749	0.6018	0.6110	0.6288	0.7216	0.6486	0.7569	0.6737	0.8243	0.8376	0.6448	0.5759	0.6707	0.5797	0.7493	0.7640
ADASYN	0.5188	0.5073	0.4750	0.5986	0.6128	0.6292	0.7150	0.6508	0.7612	0.6708	0.8301	0.8403	0.6357	0.5781	0.6728	0.5783	0.7542	0.7653
Synthpop	0.3984	0.3857	0.4195	0.4692	0.4476	0.4657	0.5793	0.5415	0.6026	0.5825	0.6419	0.6380	0.5123	0.4758	0.5368	0.5031	0.5626	0.5674
Copula	0.4430	0.4098	0.4025	0.4871	0.4483	0.4563	0.6376	0.5905	0.7132	0.5674	0.7210	0.7346	0.5669	0.5171	0.6220	0.4956	0.6292	0.6467
CTGAN	0.5088	0.5371	0.5663	0.5551	0.5937	0.6035	0.6396	0.6065	0.6923	0.5929	0.7105	0.7071	0.5776	0.5367	0.6194	0.5113	0.6358	0.6410
CopulaGAN	0.5520	0.5597	0.5520	0.5812	0.6145	0.6204	0.6730	0.6400	0.6930	0.6201	0.7279	0.7337	0.6019	0.5599	0.6243	0.5325	0.6515	0.6632
TVAE	**0.6139***	0.5760	0.6235	0.6444	0.6687	0.6778	0.7319	0.6702	0.7692	0.6913	0.8144	0.8152	0.6415	0.5793	0.6664	0.5863	0.7259	0.7314
CTABGAN+	0.5742	0.5559	0.6122	0.6413	0.6608	0.6696	0.7339	0.6698	0.7685	0.6908	0.8168	0.8188	0.6401	0.5751	0.6660	0.5851	0.7288	0.7330
TabDDPM	0.5934*	0.5758	0.6273	0.6436	0.6731	0.6799	0.7416	0.6744	0.7723	0.6936	0.8203	0.8222	0.6525	0.5822	0.6707	0.5865	0.7331	0.7383
TWAE	0.6089*	**0.6090**	**0.6326***	**0.6627**	**0.7032**	**0.7141**	**0.7563***	**0.6964**	**0.7791**	**0.7012**	**0.8358**	**0.8416**	**0.6662**	**0.6023**	**0.6838**	**0.5951**	**0.7583**	**0.7678**
Real	0.5780	0.6128	0.6285	0.6847	0.7348	0.7509	0.7535	0.7134	0.7838	0.7279	0.8662	0.8729	0.6682	0.6144	0.6896	0.6184	0.7936	0.8058

$$propensityMSE = \frac{1}{N}\sum_{i=1}^{N}\frac{(p_i - 0.5)^2}{0.25}, \tag{16}$$

where N represents the total number of records, and p_i are predicted probabilities (i.e., propensity scores) from a chosen classification algorithm. Here we use logistic regression and decision trees.

5 Results and Discussion

5.1 ML utility

In this study, we assess the performance of our proposed algorithm in comparison to other state-of-the-art (SOAT) algorithms, focusing on its machine learning (ML) utility from two distinct perspectives. Table 2 presents the average results of six classification models applied to 16 datasets, ordered in ascending order of complexity (from smallest CR to largest CI). Additionally, Table 3 showcases the performance results of all datasets for the six classification models, organized in ascending order of algorithm complexity. This dual presentation aims to comprehensively evaluate the performance of tabular data synthesis models, examining their effectiveness across different data sizes and varying levels of classification algorithm complexity. Specifically, we investigate how robust synthetic data can assist in diverse data size scenarios and contribute to the performance of

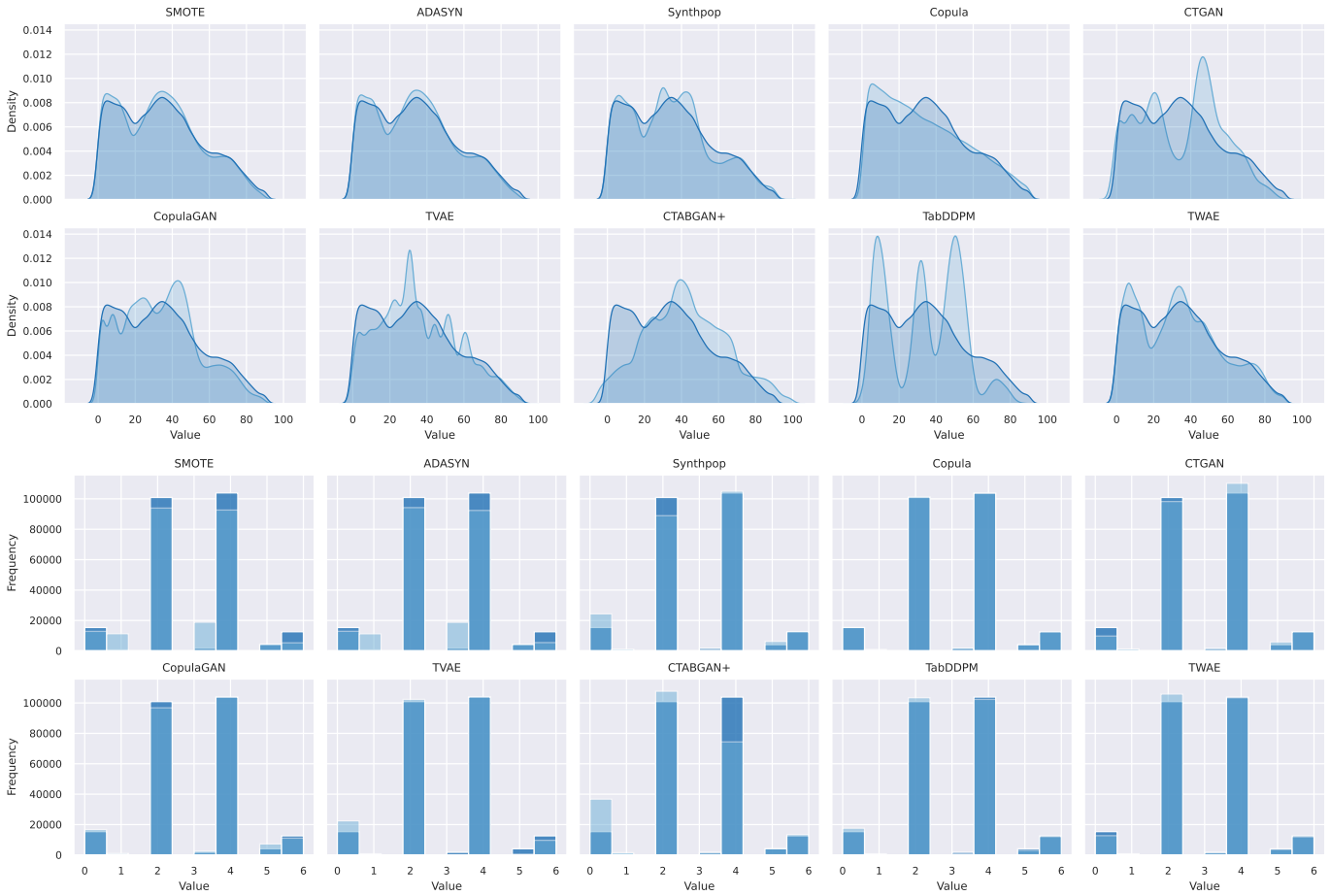

Fig. 3. Visualization of synthetic data's single column distribution v.s. the real data on the CI dataset. Upper: numerical column (*age)*; Lower: categorical column (*education*).

classification algorithms with varying levels of complexity. The benchmark for a superior synthetic dataset is its ability to demonstrate ML utility comparable to real data [6], [11].

Based on the result presented in Table 2, TWAE consistently outperforms all other algorithms across various metrics, including average F1 score, ROC-AUC, and PR-AUC. Specifically, TWAE secures the top ranking in 12 datasets with an average F1 score ranking of 1.6. Additionally, in terms of ROC-AUC, TWAE leads in 9 out of 16 datasets with an average ranking of 2.1. For PR-AUC, TWAE tops the ranking in 10 out of 12 datasets. Notably, in datasets with a more severe class imbalance (IR $>$ 4.00), including SI, NC, BM, AD, and CI, TWAE consistently achieves the highest rankings. Even in cases where TWAE does not secure the top rank, the difference in performance is minimal when compared to the best-performing algorithms. Moreover, TWAE outperforms all other algorithms on datasets with high dimensionality (>40), including JS, NO, KD, and CI. These results collectively demonstrate the superiority and robustness of TWAE against different data sizes, imbalance levels, and high-dimensionality scenarios. The enhanced robustness of TWAE can be attributed to its capability to facilitate a more meaningful and smoother interpolation between points in the latent space, which in turn results in a better-structured latent representation.

In addition to the comprehensive performance breakdown across datasets, we conducted an analysis against various classification algorithms, and the results are presented in Table 3. Overall, the proposed TWAE demonstrates superior performance over all competing data generation algorithms across all three performance metrics, with the exception of MLP when assessed using the F1 score, where it falls short compared to TVAE. Notably, MLP (0.5780 vs. 0.6089) and LR (0.6285 vs. 0.6326) trained on synthetic data generated by TWAE exhibit better performance compared to that on real data, as measured by the F1 score. This finding suggests that shallow models, such as MLP, may derive greater benefits from additional data supplementation through synthetic data.

Our extensive evaluations across diverse public benchmark datasets unveil the remarkable performance of TWAE, surpassing baseline models, including the widely recognized and challenging-to-beat shallow SMOTE model [6], [11]. Specifically, TWAE demonstrates superiority over other state-of-the-art (SOTA) methods across a majority of datasets, particularly for larger datasets. Additionally, TWAE exhibits resilience to different classification algorithms; for simpler algorithms such as MLP and LR, it even yields better results than real data. The observed improvement compared to TVAE underscores the positive impact of WAE-based architecture, the introduction of a new loss function, and the incorporation of latent space

TABLE 4
Column-wise KLD, JSD and WD. **Bold** represents the best score on each dataset, where lower indicates better

KLD	CR	SI	JS	NS	KD	EY	DE	NC	CO	LA	NO	MV	BM	AD	DB	CI	Ranking
SMOTE	0.14	0.07	0.17	0.10	0.08	0.10	0.06	0.08	0.10	0.05	0.20	0.19	0.09	0.12	0.17	0.07	5.9
ADASYN	0.13	0.07	0.17	0.10	0.08	0.09	0.06	0.08	0.10	0.04	0.20	0.19	0.09	0.12	0.17	0.07	5.3
Synthpop	0.12	0.03	0.12	0.19	**0.05**	**0.05**	0.21	0.28	0.17	0.16	0.38	**0.00**	0.10	0.21	0.16	0.27	6.9
Copula	**0.03**	**0.03**	0.09	0.11	0.06	0.12	0.13	0.20	0.13	0.02	0.33	0.05	0.08	0.16	0.12	0.11	5.6
CTGAN	0.08	0.08	**0.06**	0.08	0.07	0.08	0.13	0.07	0.07	0.10	0.25	0.08	0.06	0.09	0.07	0.08	4.1
CopulaGAN	0.06	0.09	0.10	0.10	0.08	0.07	0.11	0.08	0.08	0.09	0.23	0.12	0.07	0.08	0.06	0.08	4.6
TVAE	0.14	0.07	0.11	0.16	0.10	0.08	0.06	0.09	0.10	0.10	0.09	0.20	0.11	0.09	0.11	0.07	5.9
CTABGAN+	0.14	0.09	0.11	0.20	0.12	0.12	0.13	0.13	0.14	0.16	0.11	0.27	0.15	0.13	0.16	0.10	8.4
TabDDPM	0.13	0.08	0.11	0.17	0.10	0.09	0.09	0.10	0.11	0.12	0.09	0.22	0.13	0.10	0.14	0.07	6.3
TWAE	0.05	0.05	0.09	**0.08**	0.08	0.12	**0.03**	**0.05**	**0.03**	**0.02**	**0.07**	0.03	**0.03**	**0.03**	**0.02**	**0.03**	2.1
JSD	CR	SI	JS	NS	KD	EY	DE	NC	CO	LA	NO	MV	BM	AD	DB	CI	Ranking
SMOTE	0.17	0.08	0.13	0.07	0.05	0.09	0.03	0.04	0.08	0.01	5.05	0.23	0.06	0.08	0.13	0.03	4.3
ADASYN	0.11	0.09	0.13	0.07	0.06	0.08	0.03	0.04	0.08	0.01	5.05	0.23	0.06	0.08	0.12	0.03	4.0
Synthpop	0.28	0.02	1.37	1.50	0.25	**0.03**	2.06	4.91	2.04	0.31	6.72	**0.00**	0.07	3.75	0.84	3.99	7.8
Copula	**0.01**	**0.02**	0.25	0.17	0.08	0.42	0.22	0.31	0.14	0.01	5.38	0.04	0.14	0.19	0.32	0.16	6.2
CTGAN	0.08	0.05	**0.03**	**0.03**	**0.04**	0.04	0.14	0.03	0.03	0.04	5.08	0.04	0.03	0.04	0.03	0.03	3.1
CopulaGAN	0.03	0.06	0.71	0.08	0.04	0.04	0.39	0.06	0.11	0.04	5.08	0.33	0.07	0.05	0.11	0.04	4.8
TVAE	0.34	0.13	0.80	0.22	0.29	0.06	0.08	0.08	0.13	0.17	0.13	1.27	0.39	0.18	0.31	0.08	6.5
CTABGAN+	0.26	0.19	0.88	0.54	0.50	0.12	0.21	0.20	0.31	0.46	0.17	1.60	0.52	0.32	0.62	0.11	8.7
TabDDPM	0.24	0.15	0.81	0.42	0.30	0.07	0.13	0.14	0.19	0.20	0.12	1.40	0.44	0.19	0.54	0.08	7.3
TWAE	0.02	0.06	0.18	0.06	0.09	0.09	**0.01**	**0.02**	**0.01**	**0.00**	**0.06**	**0.00**	**0.01**	**0.01**	**0.00**	**0.01**	2.3
WD	CR	SI	JS	NS	KD	EY	DE	NC	CO	LA	NO	MV	BM	AD	DB	CI	Ranking
SMOTE	0.25	0.05	**0.03**	0.22	0.10	**0.05**	0.08	0.26	0.12	0.10	3.32	0.05	0.14	0.28	0.06	0.14	4.3
ADASYN	0.24	0.05	**0.03**	**0.21**	0.10	**0.05**	0.08	**0.24**	0.13	0.10	3.32	0.05	0.15	0.28	0.06	0.14	4.3
Synthpop	0.25	0.04	0.09	0.34	0.10	0.08	0.44	2.33	0.39	0.64	3.47	**0.00**	0.14	1.01	0.35	2.54	8.2
Copula	**0.03**	**0.01**	0.44	0.35	**0.07**	0.12	0.10	1.66	0.43	**0.01**	3.38	0.10	0.15	0.44	0.21	0.86	6.8
CTGAN	0.10	0.06	0.06	0.24	0.11	0.06	0.38	0.46	0.10	0.18	3.34	0.07	0.09	0.36	0.11	0.25	5.8
CopulaGAN	0.09	0.05	0.07	0.22	0.11	0.07	0.55	0.47	0.11	0.16	3.33	0.08	0.10	0.17	0.06	0.23	5.4
TVAE	0.16	0.03	0.08	0.44	0.08	0.06	0.04	0.98	0.10	0.10	0.08	0.13	0.09	0.24	0.11	0.23	4.4
CTABGAN+	0.19	0.04	0.07	0.63	0.10	0.10	0.13	1.18	0.20	0.23	0.10	0.18	0.16	0.36	0.19	0.42	7.8
TabDDPM	0.17	0.03	0.07	0.54	0.09	0.07	0.08	0.98	0.14	0.13	0.07	0.15	0.11	0.28	0.15	0.25	5.8
TWAE	0.06	0.02	0.06	0.22	0.08	0.11	**0.02**	0.55	**0.04**	0.02	**0.04**	0.02	**0.03**	**0.11**	**0.02**	**0.09**	2.3

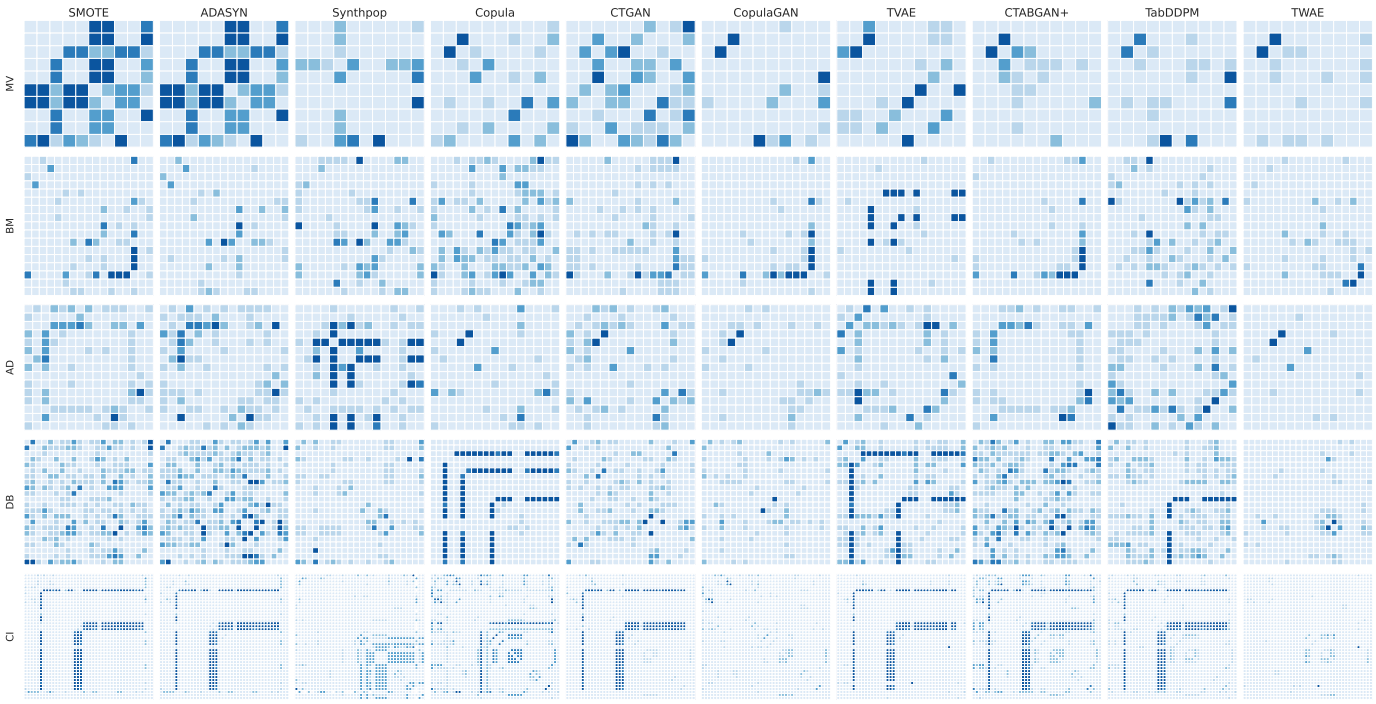

Fig. 4. Heatmaps of the pair-wise column correlation of the synthetic data v.s. real data for the top 5 largest datasets. The value represents the absolute divergence between the real and estimated correlations (the lighter, the better).

TABLE 5
Pair-wise column correlation score (p-value). **Bold** represents the best score on each dataset, where higher indicates better. TWAE gives consistently high scores, indicating the synthetic data resembles real data well.

	CR	SI	JS	NS	KD	EY	DE	NC	CO	LA	NO	MV	BM	AD	DB	CI	Average	Ranking
SMOTE	**0.34**	0.00	0.00	**0.89**	0.00	0.00	**0.31**	**0.89**	0.00	0.59	0.00	0.00	0.13	0.00	0.00	0.15	0.21	3.8
ADASYN	0.02	0.00	0.00	**0.89**	0.00	0.00	0.14	0.77	0.00	0.81	0.00	0.00	0.19	0.00	0.00	0.20	0.19	3.8
Synthpop	**0.34**	0.00	0.00	0.06	0.00	**0.34**	0.00	0.00	0.00	0.01	0.00	0.47	0.02	0.00	0.00	0.00	0.08	4.7
Copula	0.00	0.00	0.00	0.01	0.00	0.00	0.00	0.00	0.00	0.00	0.00	0.28	0.00	0.00	0.00	0.00	0.02	5.8
CTGAN	0.00	0.03	0.00	0.00	0.00	0.01	0.00	0.01	0.25	0.00	0.00	0.04	0.00	0.06	0.23	0.00	0.04	5.0
CopulaGAN	0.00	**0.04**	0.00	0.19	0.00	0.16	0.00	0.01	0.02	0.02	0.00	0.09	0.00	0.34	0.14	0.00	0.11	4.2
TVAE	0.00	0.00	0.00	0.00	0.00	0.01	0.01	0.13	0.02	0.59	0.00	0.04	0.00	0.62	0.00	0.00	0.09	4.3
CTABGAN+	0.00	0.00	0.00	0.00	0.00	0.00	0.04	0.13	0.34	0.81	0.00	0.02	0.01	0.34	0.00	0.00	0.11	4.2
TabDDPM	0.00	0.00	0.00	0.00	0.00	0.00	0.00	0.09	0.25	0.59	0.00	0.04	0.02	0.62	0.00	0.00	0.12	4.3
TWAE	0.00	0.00	0.00	0.00	0.00	0.27	0.01	0.77	**0.70**	**0.81**	0.00	**0.56**	**0.77**	**0.67**	**0.31**	**0.23**	**0.34**	**2.2**

TABLE 6
Comparison of density and coverage scores. **Bold** represents the best score on each dataset. Higher values indicate better results. TWAE gives consistently high density scores, indicating the synthetic data covers a wide range of the real distribution.

Density	CR	SI	JS	NS	KD	EY	DE	NC	CO	LA	NO	MV	BM	AD	DB	CI	Average	Ranking
SMOTE	0.49	**1.16**	4.17	0.84	0.37	0.87	0.84	0.75	0.48	1.09	0.00	0.27	0.68	0.16	1.30	0.40	0.87	6.0
ADASYN	0.51	1.15	4.11	0.85	0.36	0.87	0.84	0.75	0.48	1.08	0.00	0.27	0.68	0.16	1.29	0.39	0.86	6.2
Synthpop	0.25	0.97	0.13	0.82	0.04	0.72	0.17	0.05	0.53	0.34	0.00	1.01	0.48	0.01	0.45	0.00	0.37	8.1
Copula	0.53	0.70	0.00	0.38	0.02	0.66	0.10	0.01	0.02	0.50	0.00	0.26	0.31	0.00	0.20	0.00	0.23	9.1
CTGAN	0.41	0.29	0.01	0.66	0.08	0.60	0.14	0.54	0.52	0.79	0.00	0.74	0.75	0.61	0.84	0.58	0.47	7.4
CopulaGAN	0.46	0.27	6.51	0.49	0.05	0.92	0.21	0.38	0.99	0.81	0.00	0.88	0.70	0.54	1.00	0.44	0.92	6.7
TVAE	2.65	0.98	7.29	2.36	1.49	1.09	0.90	1.47	0.93	1.08	0.44	1.05	1.09	1.19	1.94	0.98	1.68	4.2
CTABGAN+	2.82	1.09	7.93	**2.70**	**1.56**	**1.22**	1.02	1.83	1.03	1.21	0.72	**1.15**	1.14	1.27	2.08	1.33	1.88	2.1
TabDDPM	2.67	1.04	8.29	2.56	1.54	1.17	**1.03**	1.72	1.00	1.18	0.77	1.11	**1.15**	1.31	2.07	1.29	1.87	2.5
TWAE	**3.22**	1.09	**9.00**	2.69	1.37	1.14	1.01	**2.81**	**1.11**	**1.41**	**0.98**	1.04	1.13	**1.53**	**2.22**	**1.45**	**2.08**	1.9
Coverage	CR	SI	JS	NS	KD	EY	DE	NC	CO	LA	NO	MV	BM	AD	DB	CI	Average	Ranking
SMOTE	0.73	0.73	**1.00**	0.88	0.58	0.91	0.83	0.89	0.69	0.96	0.00	0.66	0.60	0.36	0.97	0.65	0.71	4.2
ADASYN	0.76	0.75	**1.00**	0.91	0.58	**0.93**	0.85	0.91	0.70	0.97	0.00	0.67	0.61	0.37	0.97	0.66	0.73	3.4
Synthpop	0.40	0.69	0.07	0.70	0.07	0.61	0.11	0.06	0.24	0.23	0.00	0.97	0.43	0.01	0.28	0.00	0.30	8.0
Copula	0.79	0.81	0.00	0.59	0.06	0.48	0.12	0.02	0.01	0.71	0.00	0.51	0.35	0.01	0.25	0.00	0.30	8.1
CTGAN	0.69	0.37	0.02	0.79	0.20	0.71	0.10	0.74	0.67	0.80	0.00	0.76	0.77	0.71	0.80	0.71	0.55	6.0
CopulaGAN	0.74	0.38	0.92	0.72	0.09	0.76	0.09	0.58	0.65	0.80	0.00	0.48	0.72	0.61	0.83	0.66	0.56	6.1
TVAE	0.96	0.69	0.86	0.80	**0.60**	0.78	0.55	0.79	0.61	0.69	0.53	0.24	0.50	0.81	0.53	0.84	0.67	4.6
CTABGAN+	0.96	0.65	0.87	0.69	0.55	0.73	0.43	0.75	0.49	0.60	0.62	0.14	0.38	0.70	0.46	0.82	0.62	6.5
TabDDPM	0.95	0.67	0.86	0.78	0.59	0.77	0.50	0.80	0.56	0.67	0.71	0.19	0.45	0.78	0.50	0.89	0.67	5.2
TWAE	**1.00**	**0.84**	0.95	**0.96**	0.57	0.50	**0.93**	**0.96**	**0.98**	**0.99**	**0.77**	**0.99**	**0.97**	**0.96**	**0.98**	**0.97**	**0.89**	1.9

interpolation. Collectively, these elements contribute to the overall enhancement of VAE.

5.2 Statistical similarity

In this section, we present a thorough comparative analysis conducted across univariate, bivariate, and multivariate dimensions. Our primary objective is to compare the distribution at multiple levels between real and synthetic data, evaluating the ability of each data synthesis algorithm to capture essential statistical properties. In addition to the quantitative results presented in tables, we leverage visualizations to enhance the presentation of insights. Through these analyses, we aim to offer a comprehensive overview of the strengths and weaknesses inherent in each data synthesis algorithm, considering the impact of data size.

5.2.1 Univariate

At the univariate level, synthetic data generated by TWAE demonstrates the closest resemblance based on various distance metrics, including Kullback-Leibler divergence (KLD=2.1), Jensen-Shannon divergence (JSD=2.3), and Wasserstein Distance (WD=2.3), as presented in Table 4. These distance metrics quantify the disparities between individual columns of real and synthetic data, providing insights into the similarity or dissimilarity of their distributions. To enhance readers' understanding of the advantages of each synthesis algorithm, paired histograms illustrating univariate statistical similarity are included in Figure 3, which reinforces these findings by demonstrating that TWAE exhibits superior proficiency in reproducing univariate distributions, as evidenced by lower KLD, JSD, and WD, especially for larger datasets. Notably, CTGAN emerges as the second-best model when measured by KLD and JSD, while SMOTE and ADASYN rank second if measured by WD. Considering the computational overhead, SMOTE appears to be a suitable choice when both accuracy and computational efficiency are crucial.

5.2.2 Bivariate

We utilize a range of correlation measures to assess bivariate relationships, as recommended in a previous study [3]. The results, as presented in Table 5, demonstrate that TWAE outperforms all other baseline methods in generating synthetic datasets with more realistic pairwise correlations (Ranking=2.2). To provide further insights into this evaluation, we present the results for the top five largest datasets in Figure 4, reinforcing TWAE's consistently superior perfor-

Fig. 5. Distance to closest record (DCR) distributions for the CI dataset with respect to the original train set. This experiment shows that the proposed method does not "copy" samples from the training set but rather generates new synthetic samples that are close to the original samples.

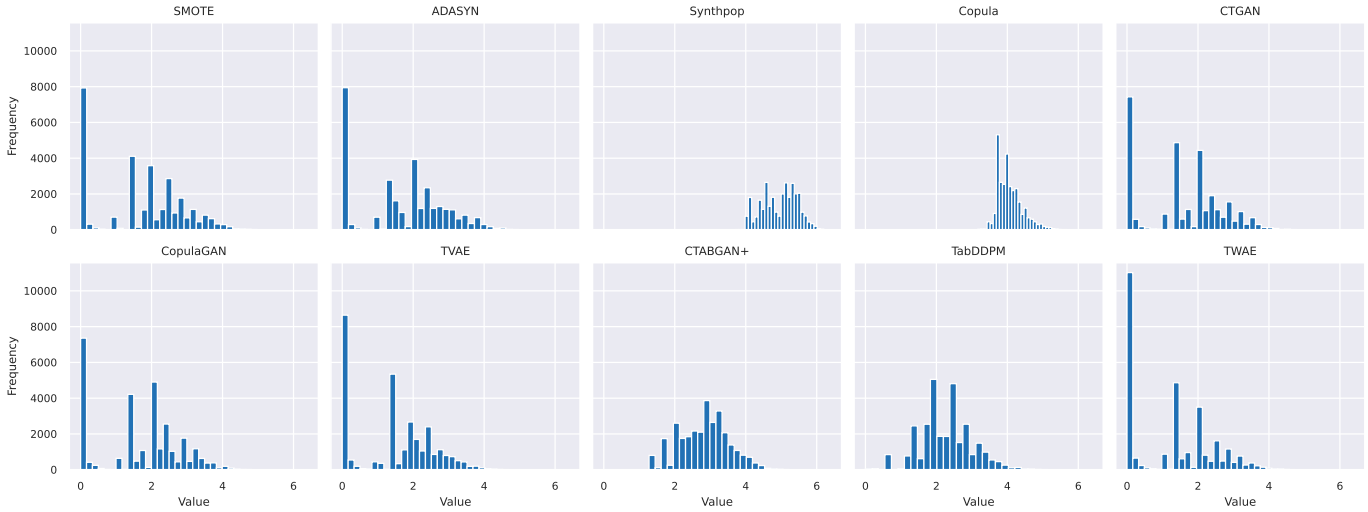

TABLE 7
Comparison of distance to closest record (DCR). **Bold** represents the best score on each dataset, where lower indicates better.

	CR	SI	JS	NS	KD	EY	DE	NC	CO	LA	NO	MV	BM	AD	DB	CI	Average	Ranking
SMOTE	2.63	0.25	1.65	1.92	1.69	0.36	0.30	2.18	0.69	0.36	9.57	0.18	0.50	0.87	1.23	1.69	1.63	4.2
ADASYN	2.60	0.24	**1.41**	1.90	1.69	**0.35**	**0.29**	2.16	0.68	0.33	9.58	0.18	0.49	0.86	1.22	1.69	1.60	3.4
SMOTENC	2.95	0.25	4.18	2.07	2.42	0.52	2.36	3.10	1.71	1.31	10.24	0.13	0.63	2.32	1.96	4.95	2.57	8.5
Copula	2.64	**0.15**	8.14	2.16	2.49	0.84	0.81	3.20	2.81	0.53	9.28	0.20	0.58	1.80	1.94	4.06	2.60	7.8
Synthpop	2.72	0.23	4.33	2.02	2.10	0.45	1.06	2.40	0.70	0.51	9.63	0.16	0.35	0.54	1.48	1.58	1.89	5.5
TVAE	2.68	0.22	3.28	2.08	2.39	0.50	1.34	2.50	0.83	0.49	9.58	0.49	0.40	0.67	1.44	1.67	1.91	6.0
CTGAN	2.36	0.33	3.33	2.00	1.71	0.49	0.38	2.33	0.83	0.70	1.34	0.75	0.77	0.52	1.70	1.48	1.31	5.1
CTABGAN+	2.37	0.35	3.32	2.08	1.75	0.54	0.46	2.36	0.97	0.82	1.23	0.79	0.87	0.62	1.75	1.51	1.36	7.1
TabDDPM	2.34	0.34	3.32	2.02	1.71	0.51	0.43	2.32	0.89	0.73	**1.12**	0.76	0.81	0.56	1.72	1.42	1.31	5.6
TWAE	**2.11**	0.23	3.27	**1.79**	**1.67**	0.50	0.38	**1.77**	**0.42**	**0.28**	1.14	**0.09**	**0.27**	**0.32**	**1.19**	**1.28**	**1.05**	**1.8**

TABLE 8
Comparison of $propensityMSE$. **Bold** represents the best score on each dataset, where higher indicates better.

	CR	SI	JS	NS	KD	EY	DE	NC	CO	LA	NO	MV	BM	AD	DB	CI	Average	Ranking
SMOTE	0.64	0.57	0.69	0.63	0.69	0.70	0.57	0.62	0.75	0.39	**1.00**	0.82	0.70	0.83	0.76	0.68	0.69	7.3
ADASYN	0.61	0.55	0.68	0.61	0.69	0.70	0.55	0.62	0.74	0.34	**1.00**	0.82	0.69	0.82	0.68	0.68	0.67	8.3
Synthpop	0.78	0.56	0.99	0.88	**0.97**	0.66	0.93	1.00	0.92	0.88	**1.00**	0.41	0.79	**1.00**	0.94	0.97	0.85	3.8
Copula	0.49	0.54	**1.00**	0.83	0.94	0.91	0.95	0.94	0.99	0.62	**1.00**	0.85	0.96	0.97	**0.97**	**0.99**	0.87	3.5
CTGAN	0.65	**0.83**	0.80	0.61	0.95	0.88	0.95	0.60	0.72	0.59	**1.00**	0.62	0.62	0.89	0.61	0.98	0.77	6.1
CopulaGAN	0.57	0.77	0.95	0.67	0.93	0.88	0.96	0.75	0.73	0.59	**1.00**	0.72	0.72	0.67	0.63	0.91	0.78	6.2
TVAE	0.68	0.61	0.97	0.76	0.91	0.86	0.84	0.69	0.74	0.67	0.99	0.89	0.89	0.69	0.93	0.75	0.81	6.5
CTABGAN+	0.70	0.65	0.98	0.83	0.93	0.89	0.87	0.75	0.81	0.73	**1.00**	0.94	0.93	0.75	0.95	0.71	0.84	3.9
TabDDPM	0.68	0.62	0.98	0.79	0.92	0.86	0.86	0.72	0.77	0.69	**1.00**	0.92	0.92	0.71	0.94	0.70	0.82	5.3
TWAE	**0.90**	0.82	0.99	**0.96**	0.94	**0.98**	**0.96**	0.97	0.94	0.85	**1.00**	**0.98**	**0.98**	0.96	0.97	0.97	**0.95**	**1.9**

mance. Similar to the observations at the univariate distribution level, TWAE excels at the bivariate level, particularly for larger datasets. However, for smaller datasets, traditional ML algorithms such as SMOTE and Synthpop demonstrate better performance. It is noteworthy that none of the algorithms successfully captured the correlations for the JS, KD, and NO datasets, which rank among the top three datasets in terms of dimensionality. This underscores a research gap in addressing bivariate relationships for high-dimensional tabular data.

5.2.3 *Multivariate*

At the multivariate level, we utilize the density score and coverage score to assess overall data fidelity and diversity, as outlined in Table 6. Once again, TWAE attains the top ranking based on the average density score, signifying its proficiency in capturing local neighborhood relationships within the generated data. The concurrent commendable performance of the other two DL-based algorithms, CTABGAN+ and TabDDPM, echoes the expected capabilities of DL algorithms in producing more realistic samples. Conversely, when considering the coverage score, TWAE maintains its position as the best-performing method, followed by SMOTE and ADASYN. This outcome aligns with expectations, given the distance metric foundations of both SMOTE and ADASYN, ensuring that the synthetic data generated remains within the bounds of the real data space. Concurrently, the lower rankings of CTGAN, CopulaGAN,

and CTABGAN+ highlight the widely recognized problem of mode collapse that is inherent in GAN-based models [25], [28]. Overall, TWAE not only excels in generating high-quality synthetic data but also demonstrates comprehensive coverage of data diversity within the real data space.

5.3 Privacy

From a privacy perspective, TWAE takes the lead in the DCR (1.8), according to Table 7, indicating that the synthetic data generated by TWAE closely resembles the real dataset, which enables its exceptional ML utility. Figure 5 visually reinforces this result, illustrating that synthetic data generated by TAWE achieves the shortest average DCR. On the other hand, as indicated in Table 8, TWAE ranks in the top in $propensityMSE$ (1.9), suggesting that simple ML algorithms can effectively distinguish between real and synthetic data. This finding implies that our synthetic data exhibits sufficient dissimilarity to prevent a straightforward replication of the real data. Overall, these evaluations demonstrate that TWAE is a versatile and effective solution compared to other baselines, producing synthetic data of superior quality and demonstrating resilience against privacy attacks.

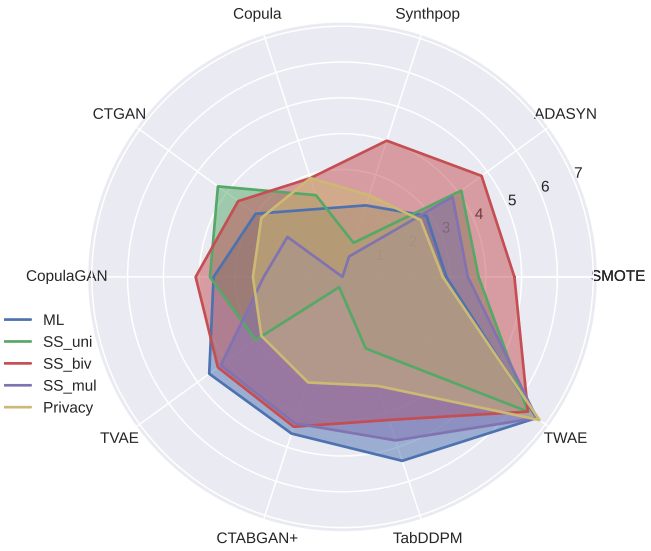

Fig. 6. Comparative analysis of data synthesis algorithms across various evaluation metrics.

For improved readability and ease of interpretation, we have consolidated the algorithm rankings across ML utility, statistical similarity at univariate, bivariate, and multivariate levels, as well as privacy, into a radar plot, illustrated in Figure 6. To construct this representation, we averaged the rankings of F1-score, AUC-ROC, and PR-AUC from Table 2 for ML utility. For univariate testing, we computed the average rankings of KLD, JSD, and WD from Table 4. In bivariate testing, the rankings are based on correlation values from Table 5. For multivariate testing, the rankings are derived from density and coverage scores in Table 6. Finally, we averaged the rankings of DCR and $propensityMSE$ from Tables 7 and 8.

In this visualization, algorithms closer to the center exhibit weaker performance, while those farther away showcase stronger performance. This concise graphical approach facilitates a quick assessment of each algorithm's strengths across multiple metrics, aiding tailored decision-making for specific business needs. It's apparent from the analysis that TWAE outperforms all other algorithms across all metrics. Moreover, DL algorithms such as TabDDPM, CTABGAN+, and TVAE perform better in ML utility, while SMOTE and ADASYN perform better in statistical similarity metrics. From the computational cost point of view, all the DL-based algorithms require significantly more time and resources to train compared to SMOTE and ADASYN. Given this, if one faces computational limitations, then ADASYN seems to strike a good balance across all metrics along with a relatively simple computational cost.

6 Conclusion

In this study, we explore the potential of WAE models for tabular data synthesis, introducing TWAE, a design adept at handling mixed data types, including both numerical and categorical features. The integration of latent space interpolation enhances the controllability and interpretability of synthetic data generation. Across various benchmark datasets, TWAE consistently outperforms existing state-of-art models, including statistical, ML, and DL approaches, in terms of ML utility, statistical similarity, and privacy preservation. The superior performance of TWAE is attributed to its novel architecture design and enhanced loss function. In conclusion, TWAE emerges as a versatile and effective solution for tabular data synthesis, positioning it as a promising choice for diverse applications across different domains. Looking ahead, our future aims include developing a novel data representation learning algorithm that leverages graph neural networks to model intricate relationships between samples, thereby advancing beyond simple latent space interpolation.

Acknowledgments

The work was supported in part by the Endeavour Fund – Smart Ideas from the New Zealand Ministry of Business, Innovation and Employment (MBIE) under contract VUW RTVU2301, the MBIE Endeavour Fund – Research Programme under contract VUW RTVU1905, and the MBIE Strategic Science Investment Fund for Data Science under contract VUW RTVU1914.

References

[1] R. Venugopal, N. Shafqat, I. Venugopal, B. M. J. Tillbury, H. D. Stafford, and A. Bourazeri, "Privacy preserving generative adversarial networks to model electronic health records," *Neural Networks*, vol. 153, pp. 339–348, 2022.

[2] M. Hernandez, G. Epelde, A. Alberdi, R. Cilla, and D. Rankin, "Synthetic data generation for tabular health records: A systematic review," *Neurocomputing*, vol. 493, pp. 28–45, 2022.

[3] A. X. Wang, S. S. Chukova, A. Sporle, B. J. Milne, C. R. Simpson, and B. P. Nguyen, "Enhancing public research on citizen data: An empirical investigation of data synthesis using Statistics New Zealand's integrated data infrastructure," *Information Processing & Management*, vol. 61, no. 1, p. 103558, 2024.

[4] V. Borisov, T. Leemann, K. Seßler, J. Haug, M. Pawelczyk, and G. Kasneci, "Deep neural networks and tabular data: A survey," *IEEE Transactions on Neural Networks and Learning Systems*, 2022.

[5] S. James, C. Harbron, J. Branson, and M. Sundler, "Synthetic data use: exploring use cases to optimise data utility," *Discover Artificial Intelligence*, vol. 1, no. 1, p. 15, 2021.

[6] R. Shwartz-Ziv and A. Armon, "Tabular data: Deep learning is not all you need," *Information Fusion*, vol. 81, pp. 84–90, 2022.

[7] S. B. Rabbani and M. D. Samad, "Between-sample relationship in learning tabular data using graph and attention networks," *arXiv preprint arXiv:2306.06772*, 2023.

[8] K. Gai and S. Zhang, "Tessellating the latent space for non-adversarial generative auto-encoders," *IEEE Transactions on Pattern Analysis and Machine Intelligence*, 2023.

[9] N. V. Chawla, K. W. Bowyer, L. O. Hall, and W. P. Kegelmeyer, "SMOTE: synthetic minority over-sampling technique," *Journal of Artificial Intelligence Research*, vol. 16, pp. 321–357, 2002.

[10] J. Kim, C. Lee, Y. Shin, S. Park, M. Kim, N. Park, and J. Cho, "SOS: Score-based oversampling for tabular data," in *Proceedings of the 28th ACM SIGKDD Conference on Knowledge Discovery and Data Mining*, 2022, pp. 762–772.

[11] A. Kotelnikov, D. Baranchuk, I. Rubachev, and A. Babenko, "TAB-DDPM: Modelling tabular data with diffusion models," in *International Conference on Machine Learning*. PMLR, 2023, pp. 17 564–17 579.

[12] I. Tolstikhin, O. Bousquet, S. Gelly, and B. Schoelkopf, "A note on the evaluation of generative models," in *International Conference on Learning Representations (ICLR 2018)*, 2018, pp. 1–16.

[13] D. Dablain, B. Krawczyk, and N. V. Chawla, "DeepSMOTE: Fusing deep learning and SMOTE for imbalanced data," *IEEE Transactions on Neural Networks and Learning Systems*, pp. 1–15, 2022.

[14] T. E. Raghunathan, "Synthetic data," *Annual Review of Statistics and Its Application*, vol. 8, 2021.

[15] S. A. Assefa, D. Dervovic, M. Mahfouz, R. E. Tillman, P. Reddy, and M. Veloso, "Generating synthetic data in finance: opportunities, challenges and pitfalls," in *Proceedings of the First ACM International Conference on AI in Finance*, 2020, pp. 1–8.

[16] Y. Gorishniy, I. Rubachev, V. Khrulkov, and A. Babenko, "Revisiting deep learning models for tabular data," *Advances in Neural Information Processing Systems*, vol. 34, 2021.

[17] M. J. Chong and D. Forsyth, "Effectively unbiased fid and inception score and where to find them," in *Proceedings of the IEEE/CVF Conference on Computer Vision and Pattern Recognition*, 2020, pp. 6070–6079.

[18] A. Lampis, E. Lomurno, and M. Matteucci, "Bridging the gap: Enhancing the utility of synthetic data via post-processing techniques," *arXiv preprint arXiv:2305.10118*, 2023.

[19] D. P. Kingma and M. Welling, "Auto-encoding variational Bayes," in *International Conference on Learning Representations (ICLR)*, 2014.

[20] J. Zhao, Y. Kim, K. Zhang, A. Rush, and Y. LeCun, "Adversarially regularized autoencoders," in *International Conference on Machine Learning*. PMLR, 2018, pp. 5902–5911.

[21] C.-H. Lai, D. Zou, and G. Lerman, "Robust variational autoencoding with Wasserstein penalty for novelty detection," in *International Conference on Artificial Intelligence and Statistics*. PMLR, 2023, pp. 3538–3567.

[22] O. Bousquet, S. Gelly, I. Tolstikhin, C.-J. Simon-Gabriel, and B. Schoelkopf, "From optimal transport to generative modeling: the VEGAN cookbook," *arXiv preprint arXiv:1705.07642*, 2017.

[23] S. Kolouri, P. E. Pope, C. E. Martin, and G. K. Rohde, "Sliced Wasserstein auto-encoders," in *International Conference on Learning Representations*, 2018.

[24] M. Yi and S. Liu, "Sliced Wasserstein variational inference," in *Asian Conference on Machine Learning*. PMLR, 2023, pp. 1213–1228.

[25] L. Xu, M. Skoularidou, A. Cuesta-Infante, and K. Veeramachaneni, "Modeling tabular data using conditional GAN," in *Advances in Neural Information Processing Systems*, 2019, pp. 7335–7345.

[26] M. Arbel, A. Korba, A. Salim, and A. Gretton, "Maximum mean discrepancy gradient flow," *Advances in Neural Information Processing Systems*, vol. 32, 2019.

[27] Ł. Struski, M. Sadowski, T. Danel, J. Tabor, and I. T. Podolak, "Feature-based interpolation and geodesics in the latent spaces of generative models," *IEEE Transactions on Neural Networks and Learning Systems*, 2023.

[28] S. Mukherjee, H. Asnani, E. Lin, and S. Kannan, "ClusterGAN: Latent space clustering in generative adversarial networks," in *Proceedings of the AAAI Conference on Artificial Intelligence*, vol. 33, 2019, pp. 4610–4617.

[29] J. Fonseca and F. Bacao, "Tabular and latent space synthetic data generation: a literature review," *Journal of Big Data*, vol. 10, no. 1, p. 115, 2023.

[30] Z. Zhao, A. Kunar, R. Birke, and L. Y. Chen, "CTAB-GAN+: Enhancing tabular data synthesis," *arXiv preprint arXiv:2204.00401*, 2022.

[31] V. Borisov, K. Seßler, T. Leemann, M. Pawelczyk, and G. Kasneci, "Language models are realistic tabular data generators," in *International Conference on Learning Representations (ICLR 2023)*, 2023, pp. 1–18.

[32] H. He, Y. Bai, E. A. Garcia, and S. Li, "ADASYN: Adaptive synthetic sampling approach for imbalanced learning," in *IEEE International Joint Conference on Neural Networks (IEEE World Congress on Computational Intelligence)*. IEEE, 2008, pp. 1322–1328.

[33] A. X. Wang, S. S. Chukova, and B. P. Nguyen, "Synthetic minority oversampling using edited displacement-based k-nearest neighbors," *Applied Soft Computing*, vol. 148, p. 110895, 2023.

[34] Y. Sun, A. Cuesta-Infante, and K. Veeramachaneni, "Learning vine copula models for synthetic data generation," in *Proceedings of the AAAI Conference on Artificial Intelligence*, vol. 33, 2019, pp. 5049–5057.

[35] B. Nowok, G. M. Raab, C. Dibben *et al.*, "synthpop: Bespoke creation of synthetic data in R," *Journal of Statistical Software*, vol. 74, no. 11, pp. 1–26, 2016.

[36] A. Gupta, D. Bhatt, and A. Pandey, "Transitioning from real to synthetic data: Quantifying the bias in model," in *Synthetic Data Generation Workshop - ICLR 2021*, 2021.

[37] A. Alaa, B. Van Breugel, E. S. Saveliev, and M. van der Schaar, "How faithful is your synthetic data? sample-level metrics for evaluating and auditing generative models," in *International Conference on Machine Learning*. PMLR, 2022, pp. 290–306.

[38] Z. Zhao, R. Birke, and L. Y. Chen, "FCT-GAN: Enhancing global correlation of table synthesis via Fourier transform," in *Proceedings of the 32nd ACM International Conference on Information and Knowledge Management*, 2023, pp. 4450–4454.

[39] A. X. Wang, S. S. Chukova, and B. P. Nguyen, "Ensemble k-nearest neighbors based on centroid displacement," *Information Sciences*, vol. 629, pp. 313–323, 2023.

[40] K. El Emam, L. Mosquera, X. Fang, and A. El-Hussuna, "Utility metrics for evaluating synthetic health data generation methods: validation study," *JMIR Medical Informatics*, vol. 10, no. 4, p. e35734, 2022.

[41] C. Yan, Y. Yan, Z. Wan, Z. Zhang, L. Omberg, J. Guinney, S. D. Mooney, and B. A. Malin, "A multifaceted benchmarking of synthetic electronic health record generation models," *Nature Communications*, vol. 13, no. 1, p. 7609, 2022.

[42] T. Liu, Z. Qian, J. Berrevoets, and M. van der Schaar, "GOGGLE: Generative modelling for tabular data by learning relational structure," in *The Eleventh International Conference on Learning Representations*, 2022.

[43] Z. Zhao, A. Kunar, R. Birke, and L. Y. Chen, "CTAB-GAN: Effective table data synthesizing," in *Asian Conference on Machine Learning*. PMLR, 2021, pp. 97–112.

[44] V. S. Chundawat, A. K. Tarun, M. Mandal, M. Lahoti, and P. Narang, "A universal metric for robust evaluation of synthetic tabular data," *IEEE Transactions on Artificial Intelligence*, 2022.

[45] L. Theis, A. van den Oord, and M. Bethge, "A note on the evaluation of generative models," in *International Conference on Learning Representations (ICLR 2016)*, 2016, pp. 1–10.

[46] L. Li, H. He, and J. Li, "Entropy-based sampling approaches for multi-class imbalanced problems," *IEEE Transactions on Knowledge and Data Engineering*, 2019.

[47] A. Goncalves, P. Ray, B. Soper, J. Stevens, L. Coyle, and A. P. Sales, "Generation and evaluation of synthetic patient data," *BMC Medical Research Methodology*, vol. 20, pp. 1–40, 2020.

[48] M. F. Naeem, S. J. Oh, Y. Uh, Y. Choi, and J. Yoo, "Reliable fidelity and diversity metrics for generative models," in *International Conference on Machine Learning*. PMLR, 2020, pp. 7176–7185.

[49] M. Platzer and T. Reutterer, "Holdout-based fidelity and privacy assessment of mixed-type synthetic data," *arXiv preprint arXiv:2104.00635*, 2021.

[50] A. Torfi, E. A. Fox, and C. K. Reddy, "Differentially private synthetic medical data generation using convolutional GANs," *Information Sciences*, vol. 586, pp. 485–500, 2022.

[51] M.-J. Woo, J. P. Reiter, A. Oganian, and A. F. Karr, "Global measures of data utility for microdata masked for disclosure limitation," *Journal of Privacy and Confidentiality*, vol. 1, no. 1, 2009.
[52] S. Hediger, L. Michel, and J. Näf, "On the use of random forest for two-sample testing," *Computational Statistics & Data Analysis*, vol. 170, p. 107435, 2022.

Alex X. Wang received his M.Sc. degree in 2020 from the School of Mathematics and Statistics, Victoria University of Wellington, New Zealand, where he is currently pursuing a Ph.D degree in Data Science. He currently works as a lead researcher on an research project on the Integrated Data Infrastructure (IDI) in Statistics New Zealand, exploring the application of data synthesis to social data. His research interests include data-centric AI, tabular data synthesis, and applications of explainable AI to social data.

Binh P. Nguyen is currently a Senior Lecturer in Data Science at the School of Mathematics and Statistics at Victoria University of Wellington (VUW), New Zealand. Prior to joining VUW in 2018, he was a Scientist at the Institute of High Performance Computing, which is part of the Agency for Science, Technology and Research (A*STAR), Singapore. Before that, he worked as a Research Fellow in the Department of Mechanical Engineering at the National University of Singapore (NUS) and then as a Research Fellow at the Centre for Computational Biology, Duke-NUS Medical School, Singapore. Dr. Nguyen earned his Ph.D. degree in Electrical and Computer Engineering from NUS. He received his B.Eng. (Hons.) and M.Sc. degrees from Hanoi University of Science and Technology, Vietnam, where he was also a Lecturer at the School of Information and Communication Technology until 2007.